JOURNAL OF MATERIALS SCIENCE 19 (1984) 3649–3657

Mechanical and structural characterization of the Nicalon silicon carbide fibre

G. SIMON, A. R. BUNSELL
Ecole Nationale Supérieure des Mines de Paris, Centre des Matériaux, B.P. 87, 91003 Evry Cédex, France

The Nicalon SiC fibre offers the possibility of the development of composite materials for use above 1000° C. This study has compared two types of Nicalon fibre, one which was shown to be amorphous and the other microcrystalline with a SiC grain radius of 1.7 nm. Both fibres behaved in a brittle manner when tested in air and in argon up to 1300° C and their strengths fell above 1000° C. There were indications that new defects were created in the amorphous fibre when tested in air above 1000° C. The microstructural analysis showed that as well as SiC, both SiO_2 and free carbon were present in both fibres. The segregations of free carbon had a mean radius of 2.0 nm in the amorphous fibre and were grouped into two populations of 1.5 and 2.2 nm in the microcrystalline fibre.

1. Introduction

The development of the Nicalon fibres by Nippon Carbon is exciting considerable interest as it offers the possibility of developing a new generation of composites for use at high temperatures. The fibre, for which Nicalon is a trade name given by its manufacturer, Nippon Carbon, consists primarily of SiC although the presence of other phases considerably influences its behaviour. It is the use of this fibre above 1000° C and its reinforcement of high temperature ceramics which is particularly appealing as it makes possible the development of ceramics with greater tenacity than those which exist at present. This would present many advantages, for example, in increasing the efficiency of diesel engines [1].

This type of fibre was developed in Japan by Yajima and his colleagues and the first publications date from 1976 [2–4]. The fibre was produced in an analogous fashion to the pyrolysis of polyacrylonitrile fibre to make carbon fibre. An organometallic precursor fibre is pyrolysed to give a predominantly silicon carbide fibre. Nippon Carbide began making available their Nicalon fibre in 1980 and since then several authors have studied the behaviour of composites reinforced with these fibres [5, 6]. Very little has appeared in the scientific literature on the microstructure and mechanical properties of the fibre, particularly when it is exposed to high temperatures. This is no doubt due to the difficulty of testing a fibre with a mean diameter of 15 μm at temperatures above 1000° C. This paper is concerned with just such a study made on two batches of Nicalon fibre which the manufacturer made deliberately with different microstructures. Unless otherwise stated the results in this paper refer to the commercially available fibre (NLP 101). The other fibre is referred to as NLM 102.

2. Experimental techniques

Characterization of the mechanical properties of the fibre was carried out using a Universal Fibre Testing machine the principles of which have been described elsewhere by Bunsell *et al.* [7]. The fibre is held between two jaws, one of which is either fixed or connected to a vibrator for dynamics tests, and the other is connected to load cells. The distance between the jaws is controlled by an electric motor which, in the case of creep or fatigue tests, is controlled through a servo system by the applied load. Any variation of the load on the fibre from the designed load causes the motor to start and the load on the fibre is brought back to the chosen level. The load is controlled to within ± 0.1 g. The addition of a tubular lanthanum

0022–2461/84 $03.00 + .12

chromite furnace permitted tests on fibres up to 1600° C. The length of the furnace meant that tests at high temperature had to be conducted on specimens with a gauge length of 220 mm. Tests were conducted in air and in argon.

The fibre diameter was measured using a Watson Image Shearing Eye piece mounted on an optical microscope. Whenever the broken ends could be recovered the fracture morphology was examined using a scanning electron microscope.

Several techniques have been used to study the microstructure of the fibre. The proportion of different elements in the fibre was measured using an electron microprobe and an Auger spectrometer. These two techniques were complementary. The microprobe was incapable of measuring quantitatively the amounts of light elements in the structure but gave information on their distribution with a resolution of about $1\,\mu m^3$. The Auger spectrometer had a resolution of $10\,\mu m^2$ but allowed a quantitative measurement to be made.

The microstructure and crystallinity of the fibre were examined by X-ray diffraction, small-angle scattering and dark-field transmission electron microscopy. Specimens for this latter technique were prepared using an ultra microtome with a diamond cutting edge.

3. Tensile behaviour

3.1 Influence of gauge length

A considerable number of fibres were tested in simple tension in order to determine the spread of properties and the influence of gauge length on strength. Fig. 1 shows the results of 100 tests at 24° C using a gauge length of 220 mm. There was considerable scatter. This type of scatter is not unusual with fibres and ceramics and is usually due to defects at the surface or in the bulk of the material. If the defects are of the same type differing only in size and are spread randomly over the fibre length the failures obey a Weibull distribution. The Weibull analysis describes the probability of survival, P_S, of the specimen at a given stress, σ, as a function of its volume, V_{50}, i.e.

$$P_S = \exp\left[-\int \left(\frac{\sigma - \sigma_u}{\sigma_0}\right)^m dV\right]. \quad (1)$$

In the case of a cylindrical fibre of uniform diameter loaded in tension, Equation 1 can be rewritten as:

$$P_S = \exp\left[-V\left(\frac{\sigma - \sigma_u}{\sigma_0}\right)^m\right], \quad (2)$$

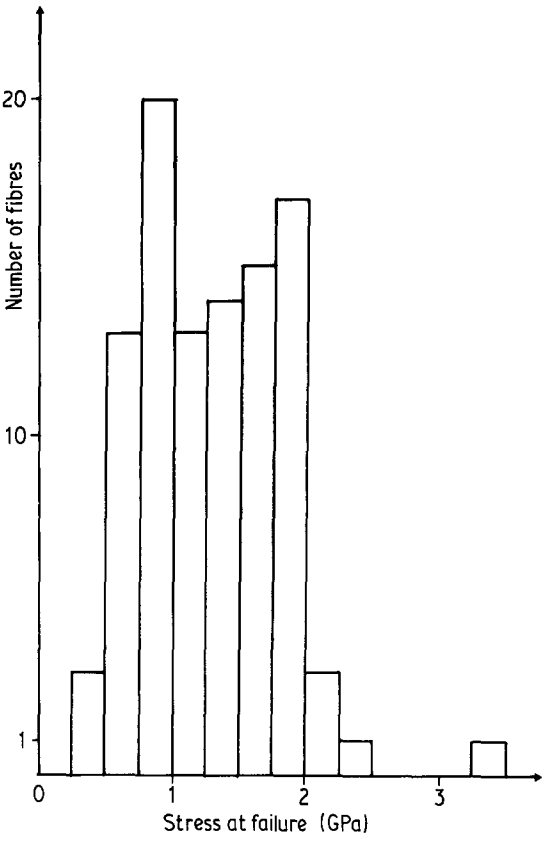

Figure 1 Failure stress histogram for the NPL 101 fibres tested at 24° C with a gauge length of 200 mm. One hundred specimens were tested and the mean failure stress was 1.29 GPa.

where σ_u is the stress at which there is never failure and is usually considered to be zero; σ_0 is a constant for the material; m is the Weibull shape parameter and characterizes the dispersion of the failure stresses. The smaller the value of m the greater the dispersion.

Equation 2 can be rewritten as:

$$\ln \ln \frac{1}{P_S} = \ln V + m \ln \sigma - m \ln \sigma_0,$$

so that for a given length

$$\ln \ln \frac{1}{P_S} = m \ln \sigma + 2 \ln D + \text{constant}, \quad (3)$$

where D is the fibre diameter.

The median stress value, corresponding to a 50% failure probability ($P_S = 0.5$), of a fibre bundle of a given length, l, can be written as a function of the volume:

$$\ln \ln \frac{1}{0.5} = \ln V + m \ln \sigma_{50} - m \ln \sigma_0$$

TABLE I Results of tensile tests on the NLP 101 fibres tested at 24° C

Gauge length (mm)	σ_R (GPa)	σ_{50} (GPa)	Standard deviations (GPa)	Weibull shape parameter, m	Young's modulus (GPa)	Standard deviations (GPa)
220	1.29	1.27	0.51	3.1	147	36
80	1.58	1.51	0.47	3.0	113	23
25	1.84	1.80	0.39	2.3	134	23
15	2.04	1.92	0.54	2.2	185	50

$$\ln \ln \frac{1}{0.5} = \ln l + 2\ln D + m \ln \sigma_{50} + \text{constant}.$$

Assuming that the average fibre diameter from one batch of specimens is the same as that from another batch we can write:

$$\ln \sigma_{50} = \frac{1}{-m} \ln l + \text{constant}. \quad (4)$$

In the case of a Gaussian or symmetrical distribution of the failure stresses around the average we would find $\bar{\sigma} = \sigma_{50}$. That was not the case as can be seen from Table I for the NLP 101 fibre and from Table II for the NLM 102 fibres; however, the differences were slight.

Therefore, it is possible to determine the Weibull shape parameter from both a series of tensile tests with fibres of all the same gauge length or by conducting tensile tests on specimens of different gauge lengths. In the former case a plot of $\ln \ln (1/P_S) - 2\ln D$ as a function of $\ln \sigma$ should give a straight line of gradient m. In the latter case a plot of $\ln \sigma_{50}$ as a function of $\ln l$ for several gauge lengths should also give the value of m.

The first approach gives information on the type of defect in the material and in particular whether there is a bi- or multimodal distribution of defects which would be shown by a change in gradient. The second approach allows the median stress value to be determined for any gauge length.

Tests were conducted with different gauge lengths. One hundred NLP 101 fibres were tested with a 220 mm gauge length, 20 at 80 mm, 30 at 25 mm and 30 at 15 mm. All fibres were taken randomly from the same bundle. The initial 100 tests with a 200 mm gauge lengths revealed that the average value of failure stress corresponded very closely (less than 10% variation) to that calculated after 30 tests. For that reason 30 specimens only were used at the other gauge lengths.

The NLP 102 fibres were tested with two gauge lengths only, 25 and 220 mm.

It can be seen from Fig. 2 that the spread of results obtained at 24° C for the NLP 101 fibres with 100 specimens 200 mm long, gave a straight line when $\ln \ln (1/P_S) - 2\ln D$ was plotted against $m \ln \sigma_r$. From this it can be seen that only one defect population existed and the Weibull shape parameter was calculated to be 3.1. Fig. 3 shows the results of plotting $\ln \sigma_{50}$ as a function of $\ln l$ for both the NLP 101 and the NLM 102 fibres and are compared with those obtained by Andersson and Warren [8] on a pre-production batch of fibres. The Weibull shape parameter calculated in this way was found to be 6.4 for the NLP 101 fibres and 8.8 for the NLM 102 fibres.

3.2. Influence of temperature

Tensile tests were conducted over a wide range of temperatures using a gauge length of 200 mm and were conducted both in air and argon with the NLP 101 fibres but in air only with the NLM 102 fibres. The results of these tests are shown in Tables III and IV. At least 30 fibres were broken at each temperature. Fig. 4 shows the variation of strengths as a function of temperature. It can be

TABLE II Results of tensile tests on NLM 102 fibres tested at 24° C

Gauge length (mm)	σ_R (GPa)	σ_{50} (GPa)	Standard deviations (GPa)	Weibull shape parameter, m	Young's modulus (GPa)	Standard deviations (GPa)
25	1.49	1.37	0.64	2.7	144	57
220	1.16	1.07	0.42	3.6	130	62

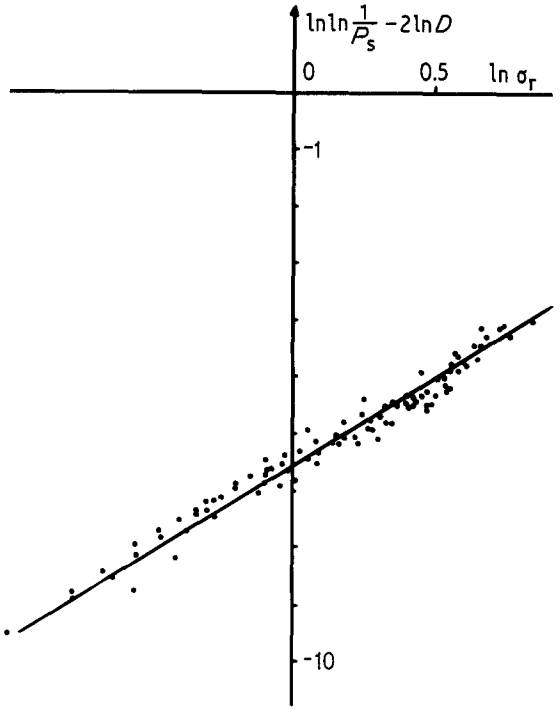

Figure 2 The fibre failures detailed in Fig. 1 were seen to be described by Weibull statistics and obey Equation 3 giving a shape parameter of 3.1.

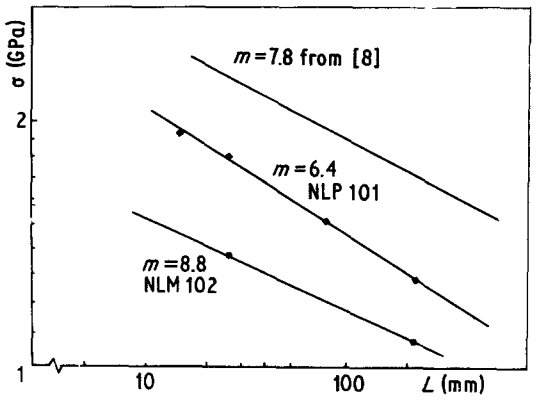

Figure 3 Variation of fibre strength as a function of gauge length. The two fibres examined in this study are compared to the preproduction results given by Andersson and Warren [8].

seen that a fall in strength occurred above 1000° C both in air and argon. The Young's moduli of the fibres was calculated after having taken into account the temperature profile across the furnace. The variation of the Young's moduli with temperature can be seen in Fig. 5. The Weibull shape parameter for the NLP 101 fibres was found not to vary from ambient to 1000° C in air and from ambient to 1300° C in argon, as shown in Fig. 6. The fall in the value of the shape parameter in air above 1000° C indicates the creation of another defect population. The shape parameter for the NLM 102 fibre was found not to change with temperature even when tests were carried out in air.

The fracture surfaces of the fibres as seen in a scanning electron microscope did not alter in appearance over the temperature range studied and were of a brittle failure. A smooth mirror zone of stable crack growth was followed by the irregular fracture surface characteristic of rapid failure. Fig. 7 shows the fracture surface of two NLP 101

TABLE III Variation of tensile properties of NLP 101 fibres over a range of temperatures and with a gauge length of 200 mm

T (°C)	Stress at failure σ (GPa)	Standard deviation, $\langle\sigma\rangle$ (GPa)	Weibull shape parameter, m	Young's modulus Y (GPa)	Standard deviation, $\langle Y\rangle$ (GPa)
24 air	1.29	0.51	3.1	147	36
650 air	1.02	0.35	3.4	127	22
800 air	0.92	0.30	3.9	111	25
argon	1.01	0.35	3.7	133	23
900 air	1.02	0.32	3.7	117	27
1000 air	1.06	0.32	3.4	97	25
argon	1.08	0.31	3.3	97	16
1150 air	0.66	0.36	1.81	85	32
argon	0.86	0.23	4.6	96	26
1300 air	0.54	0.31	1.8	95	30
argon	0.71	0.27	3.5	96	23

TABLE IV Variation of tensile properties with temperature of the NLM 102 fibres with a 220 mm gauge length

T (°C)	Breaking stress, $\bar{\sigma}_R$ (GPa)	Standard deviation, $\langle\sigma\rangle$ (GPa)	Weibull shape parameter, m	Young's modulus, E	Standard deviation, $\langle E\rangle$
24	1.16	0.42	3.6	130	42
1000	1.03	0.35	3.4	95	30
1300	0.76	0.20	3.4	88	25

fibres broken at 24° C and reveals that fracture can be initiated by internal defects. Fig. 8 shows the fracture morphology of a NLP 101 fibre broken at 1300° C in air. These photographs show no sign of plastic deformation or any surface oxide layer.

4. Structural analysis

4.1. Castaing microprobe

This technique is not well adapted to the detection of the light elements which constitute the structure of the Nicalon fibres; however, it did reveal the presence of silicon, carbon and oxygen. No other elements were detected. It was possible to determine the distribution of the elements across the fibre diameter. The zone resolution was about 1 μm^3. The three elements were found to be uniformly distributed across the diameter so that the oxygen content must have come from the cross-linking stage of fibre production which occurs in air at 200° C. Fig. 9 shows the concentration profiles for silicon, carbon and oxygen across the fibre diameter. A thin surface layer of SiO_2 on the fibre cannot be ruled out as the resolution of the technique is not sufficiently high to examine this possibility. The behaviour of the NLM 102 fibre which shows no change in Weibull shape parameter at high temperature suggests that such a layer could exist.

4.1.1. Auger spectrometry

This technique allows an analysis with an electron beam spot size of 10 μm^2 which is too great for anything other than a global measure but one which is quantitative. Auger spectrometry confirmed the existence of only three elements, silicon, carbon and oxygen in the proportions shown in Table V assuming that the three elements are in the form of SiC, C and SiO_2. These are the average values and considerable variation between individual fibres was found so that the carbon content was observed to be as high as 10% and

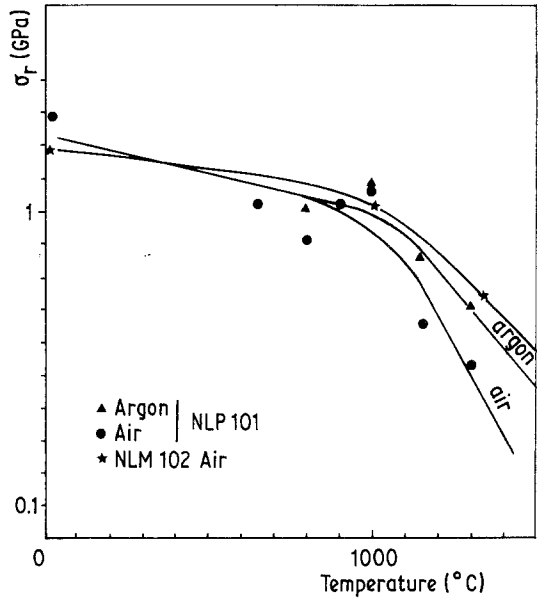

Figure 4 Variation of fibre strength with temperature.

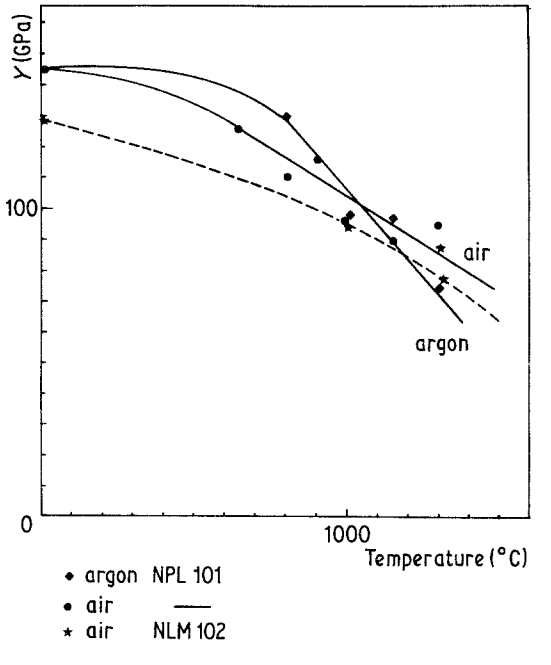

Figure 5 Variation of Young's modulus with temperature.

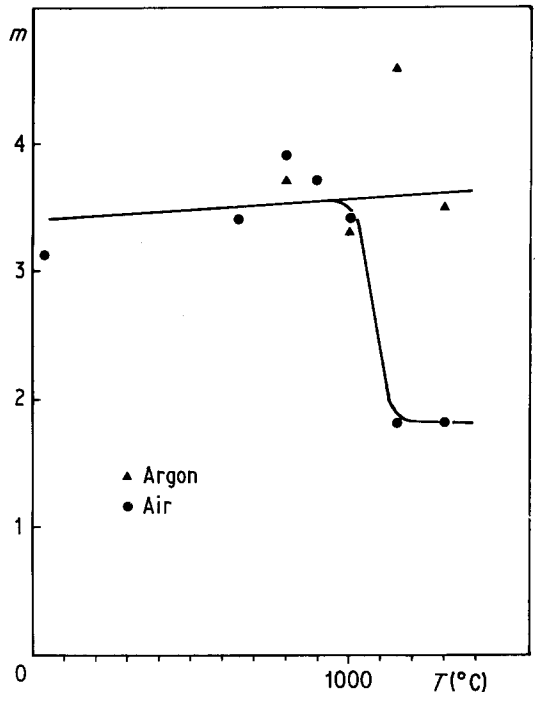

Figure 6 Variation of the Weibull shape parameter for the NLP 101 fibre tested at different temperatures.

20% by weight, respectively, in the NLP 101 and NLM 102 fibres. The figures given by Yajima *et al.* [9] for preproduction fibres were SiC 64%, C 5% and SiO_2 21%, showing that the NLM 102 fibre is closer to the original fibre than is the NLP 101.

4.2. X-ray analysis

The diffraction spectra of the two types of fibre studied are shown in Fig. 10. These results indicate that the NLP 101 fibre is amorphous. A calculation of the possible SiC β crystal size using the Scherrer method gives 1.1 nm, which seems unlikely. It is known that if the interatomic bonds are strong there is a greater likelihood of a glassy phase than a microcrystalline phase [10].

The NLM 102 fibre, however, is seen to be crystalline and the Scherrer formula gives an average diameter of 1.7 nm for the SiC β particles. This agrees with the conclusions of Yajima *et al.* [9].

There were no peaks detected corresponding to other elements, suggesting that the SiO_2 was amorphous and the carbon in a turbostatic form. Peaks would have been expected at $\theta = 2.17°$ and

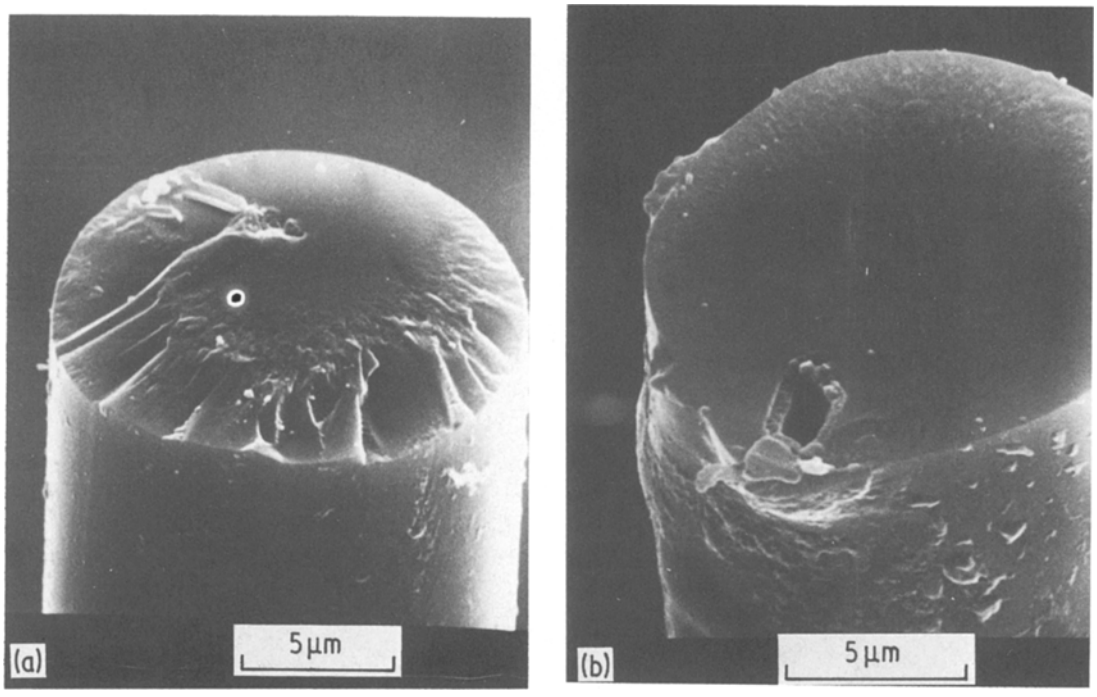

Figure 7 Fracture morphology of the NPL 101 fibre tested at 24° C, showing (a) failure initiated at the surface, and (b) failure due to an internal defect.

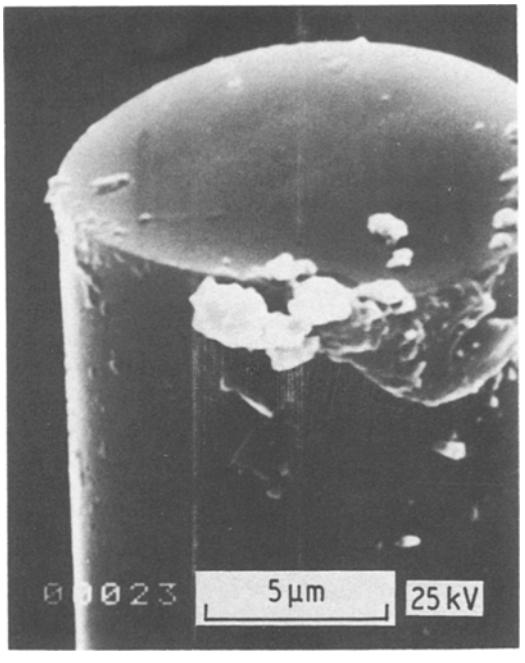

Figure 8 Fracture morphology of the NLP 101 fibre broken in air at 1300° C.

20°, respectively, and there was a slight rise in the spectral curve; however, the low percentage content of these elements means that their importance was lost in the background.

An analysis by small-angle scattering permitted a study of the possibility of segregation of carbon in the structure as its electron density is different from that of SiC and SiO_2. The gradient of the graph obtained by plotting the logarithm of the X-ray intensity as a function of ϵ^2, the square of the diffusion angle, can be related to the average particle size. These curves are shown in Fig. 11, giving an average carbon segregation radius of 2.1 nm for the NLP 101 fibre and two cluster populations of 1.5 and 2.2 nm for the NLM 102 fibre.

4.3. Transmission electron microscopy

Figs. 12 and 13 show the electron diffraction pattern and dark-field image taken from the first diffraction ring for both types of fibres. Only the presence of SiC was observed. A search for a segregation of free carbon by a dark-field study at different diffraction angles between the central beam and the first ring associated with SiC revealed nothing. There was a considerable difference found between the two fibres, confirming that the NLP 101 fibre was amorphous, showing little contrast in dark-field, and that the NLM 102 fibre was crystalline with an average crystal size of 17 μm. As the average grain size was small and the section thickness important (100 nm) it was not possible to determine the grain density as the crystals were situated at different depths in the specimen. In addition the need for an intense electron beam focusing resulted in a narrow depth of field so that while some grains are in focus others are not.

5. Discussion

The mechanical characterization of the fibres at 24° C has revealed considerable dispersion in their properties but their strength when compared to bulk silicon carbide is good, 1.3 GPa compared to 0.3 to 0.4 GPa. The Young's modulus (145 GPa) is, however, only about half that of bulk SiC ($\simeq$ 350 GPa). An analysis of these results using Weibull statistics revealed that a single defect population existed at room temperature for each fibre and accounted for the observed dispersion. The Weibull shape parameters for the two fibre types were obtained by two approaches, the first involving the testing of many fibres of the same gauge length and the second based on the variation of mean fracture stress with gauge length. These two approaches gave different values, 3 and 6.4 for the NLP 101 fibres and 3.5 and 8.8 for the NLM 102 fibres. Similar results were obtained by Andersson and Warren [8]. The most probable explanation for this difference is that the weaker fibres were broken during their removal from the bundle and so could not be tested at long gauge lengths. This leads to an over estimation of the mean fibre strength and an increase in the value of the Weibull shape parameter.

The tensile strength of both types of fibres

TABLE V Chemical make-up of the two types of Nicalon fibre tested

Fibre	SiC		C		SiO_2	
	mol %	wt %	mol %	wt %	mol %	wt %
NLP 101	65	69	20	7	15	24
NLM 102	49	63	40	15.5	11	24.5

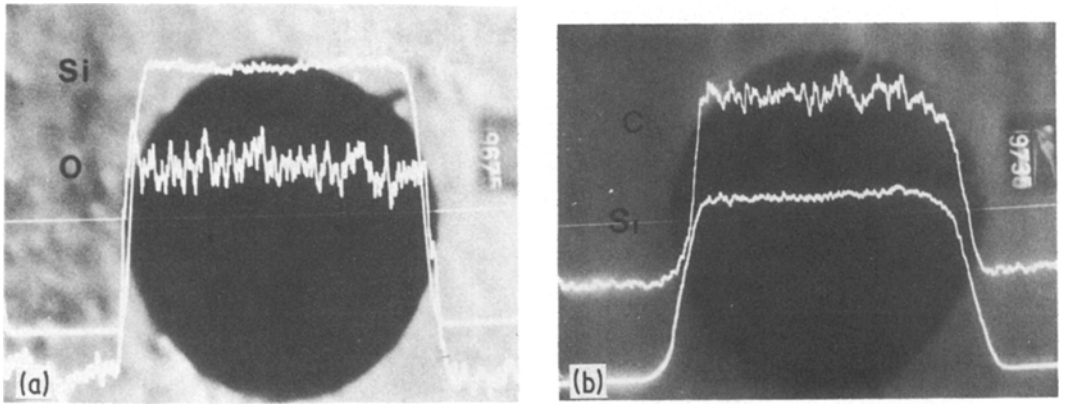

Figure 9 (a) Variation of oxygen and silicon across the diameter of a NLP 101 fibre measured by Castaing microprobe. (b) Variation of carbon and silicon across the diameter.

tested was seen to fall above 1000° C. The NLP 101 fibres showed a greater reduction in strength when tested in air than in argon. A fall in the value of the Weibull shape parameter was found to occur above 1000° C for the NLP 101 fibres tested in air, indicating the creation of new defects. No change in the appearance of the fibres was seen, however, when observed in the scanning electron microscope.

The fall in strength above 1000° C observed with the NLM 102 fibres was less than with the NLP 101 fibres and there was no change in Weibull shape parameter. The NLM 102 fibres were, therefore, seen to be the stronger of the two fibres at high temperature.

Variations of the Young's moduli of the two fibres as a function of temperature were seen to be similar. The Young's modulus was seen to decrease sooner as a function of temperature when the fibre was heated in air than was the case in argon. The fall in Young's modulus of the NLP 101 fibre tested in air was greater than when it was tested in argon.

The microstructure of the two fibres has been shown to be different; however, both contain only silicon, carbon and oxygen in the form of silicon carbide, silicon oxide (silica) and free carbon. Auger spectrometry has shown that the NLP 101 fibre contains 65% SiC and X-ray diffraction and transmission electron microscopy has shown it to be in a glassy state. The silicon oxide (15%) is

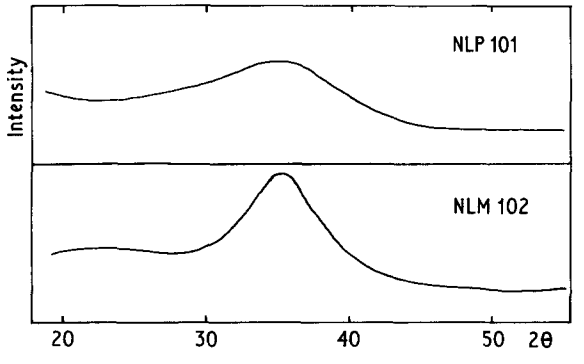

Figure 10 X-ray diffraction spectra for both fibres studied.

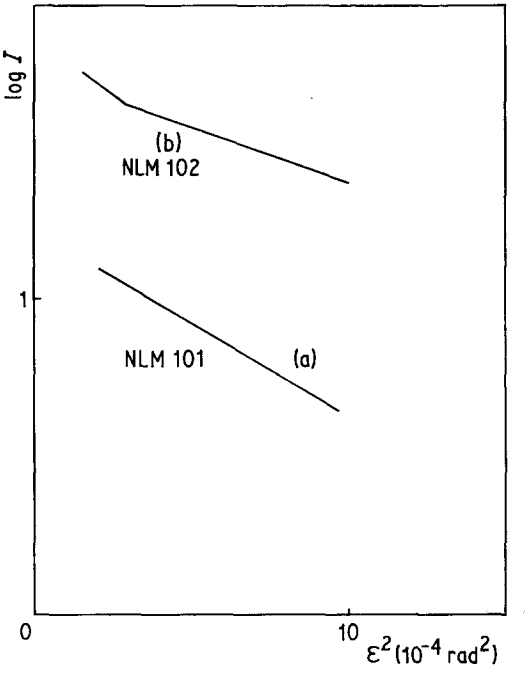

Figure 11 The plots of the X-ray diffusion intensity ($\log I$) as a function of the square of the diffusion angle (ϵ^2) reveal the average carbon segregation radii.

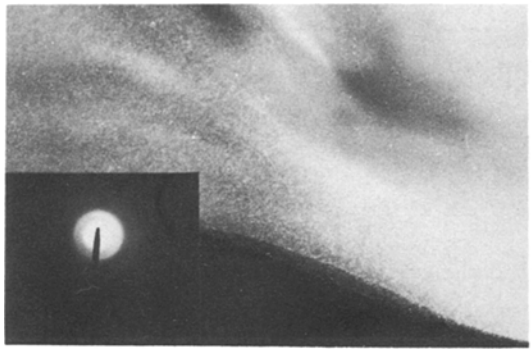

Figure 12 Dark-field micrograph of an untreated NLP 101 fibre showing it to be amorphous.

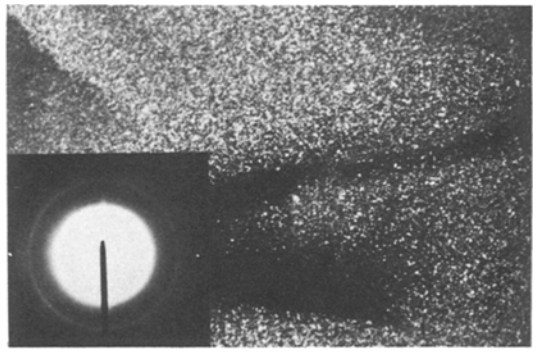

Figure 13 Dark-field micrograph of an untreated NLM 102 fibre. Average size of SiC β grains is 1.7 nm.

evenly distributed throughout the fibre and so must be a result of the cross-linking stage during fibre manufacture. Analysis by X-ray scattering has shown that free carbon is grouped in clusters of about 2.0 nm radius.

The structure of the NLM 102 fibres was found to contain different proportions of the three elements and in particular a high percentage of carbon. The SiC was found to be microcrystalline in the β form and with a grain radius of 1.7 nm. The SiO_2 was evenly distributed in the fibre and the carbon was grouped into two populations of 1.5 and 2.2 nm radii.

6. Conclusions

The tensile tests on single fibres have shown the Nicalon fibres to be brittle and that their strength distributions are described by Weibull statistics. The tests at high temperature have revealed the fall in strength above 1000° C which was more marked in the case of the NLP 101 fibres than with the NLM 102 fibres. The former fibres showed a fall in the value of the Weibull shape parameter above 1000° C revealing the creation of a new type of defect. This new defect is not, however, related to the oxidation of the free carbon as the same phenomenon is not observed with the NLM 102 fibre. The distribution of defects on the two types of fibres were similar as the Weibull shape parameters were both around 3.

The NLP 101 fibres were found to have a glassy structure whereas the NLM 102 fibres were microcrystalline. Whereas the strengths of the fibres are controlled by the size and distribution of defects, their Young's moduli must be influenced by their microstructure. The fall in Young's modulus above 900° C is likely, therefore, to be related to a marked fall in the viscosity of the SiO_2 phase.

Acknowledgements

The authors wish to thank the following people at the Institut Textile de France for their valuable assistance in the structural analysis work on the fibres. Messieurs Sotton (Director), Hagege (Assistant Director), Catoine and Mesdames Arniaud, Sonfachet. The study was in part financed by the D.G.R.S.T. Fibre samples were supplied by the S.E.P. and Nippon Carbon.

References

1. D. J. GODFREY, "The use of ceramics for engines", Proceedings of the 12th International Conference on the Science of Ceramics, Saint Vincent, Italy, 27–30 June 1983, edited by P. Vincenzini (1984) p. 27.
2. S. YAJIMA, M. OMORI, J. HAYASHI and K. OKAMURA, *Chem. Lett. (Chem. Soc. Japan)* (1976) 551.
3. S. YAJIMA, Y. HASEGAWA, J. HAYASHI and M. IIMURA, *J. Mater. Sci.* **13** (1978) 2569.
4. Y. HASEGAWA, M. IIMURA and S. YAJIMA, *ibid.* **15** (1980) 720.
5. J. J. BRENNAN and K. M. PREWO, *ibid.* **17** (1982) 2371.
6. M. DAUCHIER, P. MACICQ and J. MACE, *M.E.S. Rev. Métall.* **79**, (1982) 453.
7. A. R. BUNSELL, J. W. S. HEARLE and R. D. HUNTER, *J. Phys. E. Sci. Instrum.* **4** (1971) 868.
8. C. H. ANDERSSON and R. WARREN, in "Advances in composite materials", ICCM3, Vol. 2, edited by A. R. Bunsell, C. Bathias, A. Martrenchar, D. Menkes and G. Verchery (Pergamon, Oxford, 1980) p. 1129.
9. S. YAJIMA, K. OKAMURA, T. MATSUZAWA, Y. HASEGAWA and T. SHISHIDO, *Nature* **279** (21 June, 1979) 706.
10. G. M. BARTENEV, "The structure and properties of inorganic glasses" (Wolters-Noordhoff, Groningen, NL, 1970).

Received 30 December 1983
and accepted 24 January 1984